TOPIC REVIEW — Solid-state quantum information processing

Nuclear magnetic resonance for quantum computing: Techniques and recent achievements*

Tao Xin(辛涛)[1], Bi-Xue Wang(王碧雪)[1], Ke-Ren Li(李可仁)[1], Xiang-Yu Kong(孔祥宇)[1], Shi-Jie Wei(魏世杰)[1], Tao Wang(王涛)[1], Dong Ruan(阮东)[1], and Gui-Lu Long(龙桂鲁)[1,2,3,†]

[1] *State Key Laboratory of Low-dimensional Quantum Physics and Department of Physics, Tsinghua University, Beijing* 100084, *China*
[2] *The Innovative Center of Quantum Matter, Beijing* 100084, *China*
[3] *Tsinghua National Laboratory for Information Science and Technology, Beijing* 100084, *China*

(Received 21 November 2017; revised manuscript received 14 January 2018; published online 29 January 2018)

Rapid developments in quantum information processing have been made, and remarkable achievements have been obtained in recent years, both in theory and experiments. Coherent control of nuclear spin dynamics is a powerful tool for the experimental implementation of quantum schemes in liquid and solid nuclear magnetic resonance (NMR) system, especially in liquid-state NMR. Compared with other quantum information processing systems, the NMR platform has the advantages such as the long coherence time, the precise manipulation, and well-developed quantum control techniques, which make it possible to accurately control a quantum system with up to 12-qubits. Extensive applications of liquid-state NMR spectroscopy in quantum information processing such as quantum communication, quantum computing, and quantum simulation have been thoroughly studied over half a century. This article introduces the general principles of NMR quantum information processing, and reviews the new-developed techniques. The review will also include the recent achievements of the experimental realization of quantum algorithms for machine learning, quantum simulations for high energy physics, and topological order in NMR. We also discuss the limitation and prospect of liquid-state NMR spectroscopy and the solid-state NMR systems as quantum computing in the article.

Keywords: nuclear magnetic resonance, quantum control techniques, machine learning, topological quantum computing

PACS: 03.65.–w, 03.67.Ac, 03.67.Lx **DOI:** 10.1088/1674-1056/27/2/020308

1. Introduction

Quantum information processing (QIP) is an interdisciplinary science based on quantum mechanics, which is extremely different from the classical concepts,[1] such as wave–particle duality,[2,3] quantum entanglement,[4,5] quantum superposition.[6,7] The conceptual idea for quantum computing is originated from both the need to reduce heat dissipation[8] and efficient quantum simulation.[9,10] For instance, quantum bits are efficiently encoded based on quantum superposition principles, such as in quantum communication,[11–14] computing, and data storage.[15–17] The quantum mechanics principle makes it possible that the ability of processing and storing the data in QIP is more powerful than that of the classical counterparts. However, it is still a difficult task to implement useful QIP in practical devices. In 2000, David P. DiVincenzo proposed five requirements for the implementation of quantum computer.[18] Most importantly, the device should be a scalable physical system with well characterized qubits. So far, there are already some well-developed quantum systems that are potential to be a universal quantum processor in the future, such as nuclear magnetic resonance (NMR) system,[19] superconducting Josephson junctions,[20,21] trapped ions,[22,23] cavity QED,[24,25] optical platform,[26,27] and quantum dots.[28–30] Moreover, several systems are widely developed and employed for quantum computing in high tech companies, like Google, IBM, and D-wave. It is highly expected to become the first practical and commercial quantum computer in the near future. In this review, we restrict ourselves to the current techniques and achievements in the NMR for QIP.

The NMR is a physical phenomenon that the nuclear spins in a strong magnetic filed can absorb and emit electromagnetic radiation with resonant frequencies, which was firstly observed by Bloch and Purcell in 1946.[31] Subsequently, NMR was further developed to analyze the structure of chemical compounds in chemical science and images in medical technology. In 1998, Chuang, Laflamme, and Cory proposed NMR as a device for QIP.[32–34] In NMR,[35,36] the qubits with spin-half nuclei are selected in a chemical molecule. The chemical solvents are then placed in a magnetic field enabling a two-level energy quantum system encoded as qubits $|0\rangle$ and $|1\rangle$. The Hamiltonian of such a system is dom-

*Project supported by the National Natural Science Foundation of China (Grants Nos. 11175094 and 91221205) and the National Basic Research Program of China (Grant No. 2015CB921002).

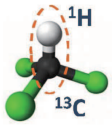
†Corresponding author. E-mail: gllong@mail.tsinghua.edu.cn

© 2018 Chinese Physical Society and IOP Publishing Ltd

inated by the Zeeman splitting and chemical shift induced by the strong magnetic field and structure of the molecule, respectively. It provides ways to distinguish spin-half nuclei in molecule at the same time. Arbitrary single-qubit rotation on the spin state can be realized by tuning the amplitudes and phases of external fields created by RF pulses. The interaction (tens to hundreds Hz in frequency) between different nuclei in the molecule provides the possibility to realize two-qubit quantum gates, such as CNOT gate. Therefore, the form of the Hamiltonian in NMR is very suitable for QIP in which any quantum unitary operations can thus be effectively implemented. For instance, a sample of ^{13}C-labeled chloroform can be used as a two-qubit quantum information processor, where the nuclear spins of ^{13}C and ^{1}H are used to encode the quantum qubits. Under the weak coupling approximation, the natural Hamiltonian of ^{13}C-labeled chloroform can be expressed as

$$\mathcal{H}^2_{\rm int} = \sum_{i=1}^{2} \omega_i \sigma_z^i + \frac{\pi J_{12}}{2} \sigma_z^1 \sigma_z^2, \tag{1}$$

where ω_i is the chemical shift of the i-th nucleus and J_{12} is the J-coupling constant between the ^{13}C and ^{1}H nuclear spins. Figure 1 shows the corresponding molecule structure and parameters. Compared with other competing quantum systems, the NMR systems with spin-half nuclei are more robust against the noise environment, and thus can be accurately controlled for quantum gates operations within the relative longer coherence time.[37]



	^{13}C	^{1}H	$T_1(s)$	$T_2(s)$
^{13}C	−7787.9		18.8	0.35
^{1}H	215.09	−3206.5	10.9	3.3

Fig. 1. (color online) Molecular structure and relevant parameters of ^{13}C-labeled chloroform. The chemical shifts (Hz) and J-coupling constant (Hz) between the different nuclei of the molecule are represented by the diagonal and off-diagonal elements of the table, respectively. The longitudinal time T_1 and transversal relaxation T_2 are also provided in the right of the table.

Recently, progresses on quantum control techniques have been obtained in NMR platform,[38,39] and the well-established techniques not only guarantee that the NMR spectrometer is capable of carrying out QIP, but also provide rich experience and guidance for the other quantum systems. Chuang *et al.* proposed composite pulses techniques in NMR[40,41] to compensate systematic errors caused by the imperfection of RF pulses, like amplitudes and frequency offsets perturbations. Realization of the frequent used rotations around the z axis is not directly available in NMR.[37] The average Hamiltonian theory is a general tool to analyze the modulation of the applied pulse sequences on the internal Hamiltonian of nuclear spins.[42] It is thus widely used to design the decoupling sequences such as WHH4 and WHH16.[43,44] Dynamical Decoupling sequence based on average Hamiltonian theory is further proposed to cancel or decrease the interaction between spins and environments, extending the coherence time of the state.[45–47] Dynamical decoupling techniques can be also combined with quantum gates for protecting quantum gate operations by simply implementing the operations between two DD sequences.[48,49] Adiabatic quantum computing can realize the evolution from the initial state to the ground state of the target Hamiltonian by slowly tuning the Hamiltonian of the systems,[50–52] which is usually used to study the properties of the ground state of many-body quantum systems. Polarization transfer technique is a common method in NMR,[53] which efficiently increases the signal-noise ratio by transferring the signal of some electron spin with high-polarization to the target nuclear spin. Techniques are further developed based on optimization search such as strongly modulating pulses (SMP)[54,55] and gradient ascent pulse engineering (GRAPE) technique.[56] However, for conditional GRAPE techniques, the calculation of the target function and gradient is completed on the classical computer, which unfortunately costs an exponential amount of time because $(2^n \times 2^n)$-dimensional matrices are inevitably involved for an n-qubit system. Recently, measurement-based quantum feedback control (MQFC) was proposed based on GRAPE technique,[57–59] which can automatically complete the calculation of the target function and gradient on a quantum information processor. Its advantage was fully demonstrated in a 12-qubit experiment on an NMR system recently. The basic principle of GRAPE and MQFC techniques will be introduced in this review since it has also been adopted in superconducting circuit[60] in addition to NMR system. Actually, Laflamme group also proposed a so-called pulse complier approach to solve the helplessness of GRAPE technique on a larger quantum system.[61,62] More ingenious quantum control techniques in NMR system were designed, for instance, the compilation method for the imperfection of selective pulses was provided to increase the control fidelity.[63] Pure-state tomography based on incomplete Pauli operators is constructed to improve the efficiency of quantum state tomography in NMR.[64]

The well-developed control techniques of NMR make it possible to realize quantum algorithms experimentally, such as Grover search algorithm,[65–67] Shor factorization algorithm,[68] Deutsch–Jozsa algorithm,[69] ordering-finding algorithm,[70] Hogg algorithm,[71] and algorithms for solving a linear equation.[72] The NMR system is a veritable and trusted quantum simulator for simulating an untrusted and uncontrolled quantum system, or an unaccessible quantum phenomena,[73] such as a quantum clock synchronization,[74] a molecular hydrogen,[75] many-body interactions,[76] localization effects,[77,78] quantum phase transition,[79,80] and quantum tunneling.[81,82] NMR quantum processor can be also

used to explore the hidden variable theory and the principle of quantum mechanics including quantum teleportation,[83] quantum dense coding,[84] wave–particle duality,[85] Bell inequality,[86,87] quantum complementarity principle,[88] and duality quantum computer.[89] Lots of research on liquid-state NMR for QIP were completed by our groups[90,91] and the collaborations with other labs such as the Institute for Quantum Computing in University of Waterloo.[92,93] It is worth to mention that non-adiabatic holonomic quantum computation was firstly experimentally realized in NMR.[94,95]

This review for techniques and achievements in NMR is organized as follows. We first introduce the general background and new-developed quantum control techniques in NMR including GRAPE and MQFC, dynamical decoupling sequences, and the approach for artificially injecting noise in NMR system. The newly-acquired achievements on topological quantum computing on NMR system are subsequently introduced. Finally, we make a summary and prospects of NMR as quantum computing, including the limitations of liquid-state NMR, the properties of solid-state NMR, and the future directions of development. For quantum control of spin systems, we recommend the book by Levitt (2008) for the basics of NMR.[96] Readers can also refer to the following literatures for NMR: Suter and Mahesh (2008)[97] and Wiseman and Milburn (2010).[98] For further literatures on quantum computing, we recommend the book by Nielsen and Chuang (2000) for the comprehensive introduction of quantum computation and quantum information.[99]

2. The well-developed techniques in NMR system

2.1. Gradient ascent pulse engineering technique

The common pulse optimization technologies based on optimized algorithm search are the strongly modulating pulse (SMP) proposed by Cory *et al.*[54,55] and gradient ascent pulse engineering (GRAPE) proposed by Glaser *et al.*[56] The GRAPE technique originated from NMR has extensive applications in QIP. The basic idea of the GRAPE method is explained in the following. For an NMR system with n-qubit, the total Hamiltonian contains the internal term and the radio frequency (RF) term $H_{\rm tot}(t) = H_{\rm int} + H_{\rm rf}(t)$,

$$\begin{aligned} H_{\rm int} &= \sum_{i}^{n} \omega_i \frac{\sigma_z^i}{2} + \sum_{1\leqslant i<j\leqslant n} \pi J_{ij} \frac{\sigma_z^i \sigma_z^j}{2}, \\ H_{\rm rf}(t) &= -\sum_{k=1}^{n} \gamma_k B_k (\cos(\omega_{\rm rf}^k t + \phi_k)\sigma_x^k \\ &\quad + \sin(\omega_{\rm rf}^k t + \phi_k)\sigma_y^k), \end{aligned} \tag{2}$$

where ω_i and J_{ij} are the Larmor frequency and the scalar coupling constant, respectively. B_k and ϕ_k are the amplitude and phase of the controlling field on the k-th nucleus. The key of the GRAPE technique is to find the optimal parameters (B_k, ϕ_k) of the RF field making the time propagator $U_{\rm T}$ (density operator $\rho_{\rm f}$) very close to the desired target evolution $U_{\rm tar}$ (desired target operator $\rho_{\rm tar}$). Assuming that the total time of the RF field is T, the total evolution time is averaged into M discrete segments and the time of each segment is $\Delta t = T/N$. The time propagator of the m-th segment can thus be expressed as

$$U_m = \exp\left[-{\rm i}\Delta t \left(H_{\rm int} + \sum_k u_x^k[m]\sigma_x^k + \sum_k u_y^k[m]\sigma_y^k \right) \right], \tag{3}$$

where $u_x^k[m]$ and $u_y^k[m]$ are the amplitude of the m-th segments of the RF field in x and y axes. So the total evolution is $U(T) = U_M U_{M-1} \cdots U_2 U_1$. The fitness function to be optimized is the distance with the target, which can be expressed as $F_{\rm u} = |{\rm tr}(U_{\rm tar}^{\dagger} U_{\rm T})|/2^n$ for the given target evolution $U_{\rm T}$ or $F_{\rm s} = {\rm tr}\left(\rho_f \rho_{\rm T}\right)$ for the given target state $\rho_{\rm T}$. The key of the GRAPE algorithm is to consider fidelity $F_{\rm u}$ and $F_{\rm s}$ as the the optimization problem of the multivariate function. In the first-order approximation, the gradients of $F_{\rm u}$ and $F_{\rm s}$ as a function of parameters $u_x^k[m]$ and $u_y^k[m]$ are

$$g_{x,y}^k[m] = \frac{\partial F_{\rm u}}{\partial u_{x,y}^k[m]} \approx -2{\rm Re}\left[U_{\rm tar}^{\dagger} U_M \cdots (-{\rm i}\Delta t \sigma_{x,y}^k) U_m \cdots U_1 \right]/2^n, \tag{4}$$

$$g_{x,y}^k[m] = \frac{\partial F_{\rm s}}{\partial u_{x,y}^k[m]} \approx {\rm tr}(-{\rm i}\Delta t U_M \cdots U_{m+1}[\sigma_{x,y}^k, U_m \cdots U_1 \rho_0 U_1^{\dagger} \cdots U_m^{\dagger}] U_{m+1}^{\dagger} \cdots U_M^{\dagger} \rho_{\rm f}). \tag{5}$$

The fitness functions can be increased in the gradient iteration as follows:

$$u_{x,y}^k[m] \to u_{x,y}^k[m] + \varepsilon \cdot g_{x,y}^k[m]. \tag{6}$$

The GRAPE procedure starts from an initial guess of input $(u_x^k[m],\ u_y^k[m])$ and then evaluates both the fitness functions and corresponding gradients, and then continues iterations until the fitness functions reach the target values.

2.2. Measurement-based quantum feedback control

The basic principle of the GRAPE technique introduced above is a process of creating a randomly initial guess, evaluating a fitness function f and a gradient g, determining a search direction, producing an iteration, and finishing an optimization. However all these procedures are performed in a classical computer. It inevitably contains the simulation of time

propagations of the controlled quantum system, which will be impracticable for a lager system with the classical computer. To improve the performance of GRAPE, MQFC as a quantum version of GRAPE technique was proposed by constructing a hybrid quantum-classical machine.[57–59] The critical point is to efficiently calculate the fitness function and the gradient on a reliable quantum simulator which can be set as the target system itself. The generation of the control parameters and the determination of the search direction in each iteration are still implemented on a classical computer. In such a way, it greatly saves the running time for optimization and improves the control fidelity.

In the following, we present the mathematical description of optimizing a control sequence with M slices $U_{\rm tot} = U_M U_{M-1} U_{M-2} \cdots U_2 U_1$ to transfer the initial state ρ_0 to the target state $\rho_{\rm f}$. Any state has the unique decomposition in Pauli basis $\rho = \sum_{i=1}^{r} c_i P_i$, where r is no more than $4^n - 1$ for a system with n-qubit, P_i is an element of the Pauli group $\{I, \sigma_x, \sigma_y, \sigma_z\}^{\otimes n}$, and c_i is the decomposed coefficient. Then the definition of fitness function f is

$$f = \text{fidelity}(U\rho_0 U^\dagger, \rho_{\rm f}) = \sum_{i=1}^{r} c_i \text{tr}(U\rho_0 U^\dagger P_i). \tag{7}$$

So the amount of measurements f directly depends on the form of the target state f. It is actually the number of r. There is no improvement on efficiency if the number of Pauli terms $r = 4^n - 1$, which is equivalent to quantum state reconstruction. However, the number of r is sometimes small, or at least polynomial for some experiments. Then the gradient function of the m-th slide of the control sequence with totally M slices can be calculated to the first order as shown in Eq. (5). We consider the homonuclear case with the following equation:

$$[\sigma^i_{x,y}, \rho] = \text{i}\left[\left(\frac{\pi}{2}\right)^i_{x,y} \rho \left(\frac{\pi}{2}\right)^{i\dagger}_{x,y} - \left(-\frac{\pi}{2}\right)^i_{x,y} \rho \left(-\frac{\pi}{2}\right)^{i\dagger}_{x,y}\right]. \tag{8}$$

We can further obtain the form of the gradient

$$\begin{aligned} g_{x,y}[m] = {} & \frac{\Delta t}{2} \sum_{i=1}^{n} \text{tr}\left[U_M \cdots U_{m+1} \left(\frac{\pi}{2}\right)^i_{x,y} U_m \cdots U_1 \rho_0 \left(U_M \cdots U_{m+1} \left(\frac{\pi}{2}\right)^i_{x,y} U_m \cdots U_1\right)^\dagger \rho_{\rm f}\right] \\ & - \frac{\Delta t}{2} \sum_{i=1}^{n} \text{tr}\left[U_M \cdots U_{m+1} \left(-\frac{\pi}{2}\right)^i_{x,y} U_m \cdots U_1 \rho_0 \left(U_M \cdots U_{m+1} \left(-\frac{\pi}{2}\right)^i_{x,y} U_m \cdots U_1\right)^\dagger \rho_{\rm f}\right]. \end{aligned} \tag{9}$$

It is clear that the measurement of gradient $g_{x,y}[m]$ can be obtained by applying a local $\pi/2$ pulse between m-th and $(m+1)$-th slices and the subsequently measuring the distance between the finial state and $\rho_{\rm f}$. In other words, $4n$ experiments are necessary for measuring $g_{x,y}[m]$ if $r = 1$. The efficiency of MQFC may be doubted when the target state $\rho_{\rm f}$ is complicated. Indeed MQFC only makes sense when we limit our considerations to special sparse states. There is of course no doubt that MQFC has advantages over traditional methods to control a lager system, as it is still difficult to precisely manipulate the dynamics of a lager system in the simplified case with current techniques.

2.3. Dynamical decoupling sequence

Dynamical decoupling technique (DD) is also derived from NMR spectrometer,[100] which is originally created to obtain a high-precision element spectrum. With the rise of quantum information science and technology, DD technique can also be used to preserve quantum information for a longer time by periodic sequences of instantaneous control pulses.[101] Therefore, it plays a very important role in the field of quantum control.

Assuming that a single-qubit quantum system with the initial state $|\psi(0)\rangle$ is only affected by the dephasing noise, the corresponding Hamiltonian model can be expressed as $H = \beta(t)\sigma_z/2$, the propagator after evolution time τ is

$$U = \exp\left[-\text{i}\int_0^\tau \text{d}t \frac{\beta(t)}{2}\sigma_z\right] = \exp\left[-\text{i}\frac{\theta(\tau)}{2}\sigma_z\right]. \tag{10}$$

It shows that the coherence of the state $|\psi(0)\rangle$ can be easily destroyed by the dephasing noise. The common approach of DD is to frequently apply π pulses to protect the coherence of the initial state. For instance, n instantaneous π pulses around the x-axis are alternately applied in the total free evolution line. $|\psi(0)\rangle$ will evolute to

$$\begin{aligned} |\psi(T)\rangle = {} & \left[\exp\left(-\text{i}\theta_n\frac{\sigma_z}{2}\right)\right]\left[\exp\left(-\text{i}\pi\frac{\sigma_x}{2}\right)\right] \\ & \times \left[\exp\left(-\text{i}\theta_{n-1}\frac{\sigma_z}{2}\right)\right] \cdots \left[\exp\left(-\text{i}\pi\frac{\sigma_x}{2}\right)\right] \\ & \times \left[\exp\left(-\text{i}\theta_1\frac{\sigma_z}{2}\right)\right]\left[\exp\left(-\text{i}\pi\frac{\sigma_x}{2}\right)\right]|\psi(0)\rangle \\ = {} & \exp\left(-\text{i}\Phi\frac{\sigma_z}{2}\right)|\psi(0)\rangle, \end{aligned} \tag{11}$$

where $\Phi = (-1)^n\theta_n + (-1)^{n-1}\theta_{n-1} + \cdots + \theta_2 - \theta_1$. It can be seen that if the noise frequency is sufficiently low and the pulses are equidistantly distributed, then $\Phi \approx 0$. Hence the quantum state approximately remains unchanged. Dynamical decoupling is to approximately average the unwanted system-environment coupling to zero. The basic principle of dynamical decoupling[102] is shown Fig. 2.

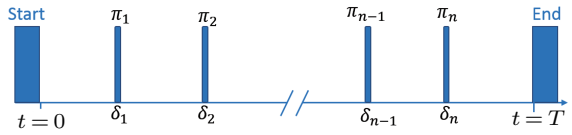


Fig. 2. (color online) Schematic representation of dynamical decoupling pulse sequences. During the evolution from $t=0$ to $t=T$, π pulses are continually applied to the protected state with different time points. Time point of $\imath\pi_i$ is labeled by the symbol δ_i.

The first DD sequence is the Hahn spin echo in the NMR system.[103] Based on the Hahn echo, periodic dynamical decoupling (PDD)[104] and CPMG[105,106] were further discovered

$$P_{\mathrm{PDD}} = E_\tau(\pi E_\tau)^n, \quad P_{\mathrm{CPMG}} = (E_\tau \pi E_\tau)^{2n}, \tag{12}$$

where E_τ is free evolution of time τ. Actually, the PDD sequence involves the repetitive application of the Hahn echo. Besides, CPMG has a very good inhibitory effect on the noise of high frequency cutoff.

In 2007, Uhrig showed that the manipulation of the relative pulse locations for fixed n and T leads to the modification of the filter function and then proposed the so-called Uhrig DD (UDD) sequence,[107,108] which achieves n-order decoupling. Different from PDD and CPMG, UDD sequence is non-equidistant in the time domain. In the sequence of time T, the time of the m-th π pulse can be written as

$$\delta_m = \sin^2\left(\frac{\pi m}{2n+2}\right). \tag{13}$$

It is concluded that UDD is more effective on noise of sharp high frequency cutoff, which has been demonstrated in solid-state NMR and ion trap systems.[109–111]

The various DD sequences mentioned above are just used to fight against dephasing noise. It is also useful to design a DD sequence that suppresses both decoherence and operational errors. To realize this purpose, Khodjasteh and Lidar proposed concatenated dynamical decoupling (CDD)[112] consisted of π pulses around X, Y, and Z axes. The iteration rule between different orders is

$$E_\tau^{n+1} = E_\tau^n X E_\tau^n Y E_\tau^n X E_\tau^n Y. \tag{14}$$

CDD can use the $O(4^n)$ pulses to simultaneously achieve n-order decoupling for the two kinds of common noises, but it will be a challenge in experiments when n becomes bigger. In 2010, Lidar *et al.* proposed quadratic UDD (QDD)[113–115] based on UDD, which guarantees simultaneous elimination of both transverse dephasing and longitudinal relaxation to n-order with only $O(n^2)$ pulses.

2.4. Artificially injecting noise technique

Noise from the environment is a double-edged sword. In some special cases, noise is unwanted that needs to be suppressed. But it also can become a crucial factor that promotes the evolution of the system to certain states yielding new phenomena.[116,117] In order to evaluate the performance of various DD sequences such as CDD, UDD, QDD under various noises or to study the dynamical evolution of the open quantum systems under some special noises, we usually artificially construct these noises in experiments which naturally exist in a controlled system. Here we introduce some methods of artificially injecting miscellaneous noises in NMR system,[47,118,119] including longitudinal relaxation noise, transverse relaxation noise, and hybrid noise.

2.4.1. Longitudinal relaxation noise

In the case where the qubits are absolutely stable, the mechanism of triggering the longitudinal relaxation of the NMR system is the revelation and amplitude fluctuation of the control field. The corresponding Hamiltonian model can be equivalently written as $H_{\mathrm{LR}}(t) = \hat{\beta}_x(t)\Omega\sigma_x$ with the Rabi rate Ω. $\hat{\beta}_x(t)\Omega$ has the following form:

$$\hat{\beta}_x(t)\Omega = \sum_{j=1}^{N} \alpha_x F(\omega_j)\sin(\omega_j t + \phi_j), \tag{15}$$

where $\alpha_i = x, y, z$ is the noise amplitude and ϕ_j is a random phase. The noise frequency ω_j is an integer multiple of a base frequency ω_0, $\omega_j = j\omega_0$. $N\omega_0$ determines the point of high-frequency cutoff, and the function $F(\omega_j)$ is the noise spectrum of this model. Then the two-time correlation function for $\beta_x(t)$ is written as

$$\langle \beta_x(t)\beta_x(t+\tau)\rangle = \frac{\omega_0^2\alpha_x^2}{2}\sum_{j=1}^{N}[F(\omega_j)]^2\cos(\omega_j\tau). \tag{16}$$

The power spectral density (PSD) can describe the energy distribution of the stochastic signals in the frequency domain. Applying the Wiener–Khintchine theorem, we then obtain the PSD by Fourier transform

$$S_\Omega(\omega) = \frac{\pi\alpha_x^2}{2}\sum_{j=1}^{N}[F(\omega_j)]^2[\delta(\omega-\omega_j)+\delta(\omega+\omega_j)]. \tag{17}$$

Hence, we can use the model of PSD to reverse the noise distribution in time domain. For instance, if we want to simulate the PSD for $S_\Omega(\omega) \sim \omega^p$, then the modulation function $F(\omega_j) = (\omega_j)^p$. The determination of $F(\omega_j)$ directly provides us the time-domain distribution of $\hat{\beta}_x(t)$. We can explore the dynamics of a quantum system with this noise model. The total Rabi rate $\Omega(t)$ will be $(1+\hat{\beta}(t))\Omega$, which indicates the undulating effect of the control field amplitude.

2.4.2. Transverse relaxation noise

Transverse relaxation noise usually puts a dephasing effect in a system, which mainly comes from the inhomogeneous and non-static magnetic field in NMR system in the classical case. Similar to the method for longitudinal relaxation noise,

$$\beta_z(t) = \sum_{j=1}^{N}\alpha_z F(\omega_j)\omega_j\cos(\omega_j t + \phi_j), \tag{18}$$

the PSD and noise spectrum $F(\omega_j)$ can be written as

$$S_z(\omega) = \frac{\pi\alpha_z^2}{2}\sum_{j=1}^{N}[F(\omega_j)\omega_j]^2[\delta(\omega-\omega_j)+\delta(\omega+\omega_j)],$$
$$F(\omega_j) = (\omega_j)^{p/2-1}. \tag{19}$$

Figure 3 shows the functional form required for $F(\omega_j)$ in order to achieve common noise PSDs.

	Dephasing				Amplitude			
	$1/f^2$	$1/f$	White	Ohmic	$1/f^2$	$1/f$	White	Ohmic
p	-2	-1	0	1	-2	-1	0	1
$F(\omega_j)$	ω_j^{-2}	$\omega_j^{-\frac{3}{2}}$	ω_j^{-1}	$\omega_j^{-\frac{1}{2}}$	ω_j^{-1}	$\omega_j^{-\frac{1}{2}}$	ω_j^{0}	$\omega_j^{\frac{1}{2}}$

Fig. 3. (color online) The functions $F(\omega_j)$ for the given noise PSDs. The different noise models are presented, including $1/f^2$, $1/f$, white, and Ohmic noises.

Under the influence of transverse relaxation noise, the initial state $|\psi(0)\rangle = \alpha|0\rangle+\beta|1\rangle$ with the Hamiltonian $\beta_z(t)\sigma_z = \hat{\beta}_z(t)\omega_L\sigma_z$ in the rotating frame after time τ will become

$$\begin{aligned}|\psi(\tau)\rangle &= \exp[-i\int_{\tau 1}^{\tau 2} dt\beta_z(t)\sigma_z/2](\alpha|0\rangle+\beta|1\rangle)\\ &= \alpha e^{-i\Delta\theta_\tau/2}|0\rangle+\beta e^{i\Delta\theta_\tau/2}|1\rangle\\ &= e^{-i\Delta\theta_\tau\sigma_z/2}|\psi(0)\rangle,\end{aligned} \tag{20}$$

where $\Delta\theta_\tau$ is integral of $\beta_z(t)$ and ω_L denotes the Larmor frequency. Hence if we attempt to simulate the evolution of a quantum system in the dephasing environment, we just rotate the angle $\Delta\theta_\tau$ along the z axis at the desired point in time.

2.4.3. Hybrid noise

Simulation of a hybrid noise cannot simply combine the two kinds of noises we mentioned above, because $\beta_x(t)\sigma_x$ does not commute with $\beta_z(t)\sigma_z$. The Hamiltonian of the system and control field with a hybrid noise in rotating frame under resonance condition $\omega = \omega_L$ is

$$H(t) = \hat{\beta}_x(t)\Omega\frac{\sigma_x}{2}+\hat{\beta}_z(t)\omega_L\frac{\sigma_z}{2}. \tag{21}$$

Considering that the rotations around z axis are not available in NMR platform, we usually transfer the above Hamiltonian to the interaction picture. The Hamiltonian in interaction picture is

$$\begin{aligned}\tilde{H}(t) &= U_z^\dagger(t)\hat{\beta}_x(t)\Omega\frac{\sigma_x}{2}U_z(t)\\ &= \exp\left[i\int_0^\tau d\tau\hat{\beta}_z(t)\omega_L\frac{\sigma_z}{2}\right]\hat{\beta}_x(t)\Omega\frac{\sigma_x}{2}\\ &\quad\times\exp\left[-i\int_0^\tau d\tau\hat{\beta}_z(t)\omega_L\frac{\sigma_z}{2}\right]\\ &= \hat{\beta}_x(t)\Omega e^{i\sigma_z\Delta\theta_\tau/2}\frac{\sigma_x}{2}e^{-i\sigma_z\Delta\theta_\tau/2}\\ &= \hat{\beta}_x(t)\Omega[\sigma_x\cos(\Delta\theta_\tau)-\sigma_y\sin(\Delta\theta_\tau)]/2.\end{aligned} \tag{22}$$

When we transfer it again to the rotating frame, the time propagator with the decoherence effect will be

$$\begin{aligned}U(t) &= \exp[-i\Delta\theta_t\sigma_z/2]\mathcal{T}\exp\left\{-i\int_{t_0}^{t} z\,d\tau\hat{\beta}_x(\tau)\Omega\right.\\ &\quad\left.\times[\sigma_x\cos(\Delta\theta_\tau)-\sigma_y\sin(\Delta\theta_\tau)]/2\right\}.\end{aligned} \tag{23}$$

In order to create a hybrid noise environment, the noise wave functions $\beta(t)$ and $\theta(t)$ are artificially created and then injected into the signal generator to modulate the control field. The qubit is rotated in the fluctuating Rabi frequency around a changing axis on the x–y plane by the control field and then rotated an angle $\Delta\theta_t$ around z axis. Therefore, we have proposed a complete approach of artificially noise in a controlled system,[38,47] which can be adapted to both NMR and other quantum systems.

3. Achievements for quantum algorithm on NMR

Quantum computation is a novel model utilizing quantum mechanical principle to realize a faster computing speed with the assistance of the superposition of quantum states different from the classical computer. Hence quantum computers can be used to solve some difficult problems that are not feasible on a classical computer. For example, finding the prime factorization of an n-bit integer is thought to require $\exp\left[\Theta(n^{1/3}\log^{2/3}n)\right]$ operations using the best classical algorithm. However, a quantum algorithm proposed by Shor[120] can accomplish the same task using $\Theta(n^2\log n\log\log n)$ operations. That is, a quantum algorithm can factor a prime number with exponentially faster speed than the best known classical algorithms.

It is well known that using classical computers to factor large numbers is extremely resource demanding, and that Shor's factoring algorithm could theoretically allow a quantum computer to factor the same numbers with fewer operations. However, although Shor's algorithm has been demonstrated in many different physical systems,[68,121–125] the largest numbers actually factored by Shor's algorithm are still only 21 and 143[125,126] until now. An alternative to Shor's algorithm relies on first transforming the numbers into a binary optimization problem and then solving it with quantum annealing. Li *et al.* reported their experiment using this method. In their work, they used the adiabatic quantum computing (AQC) technology to obtain better results in which the prime factors of 291311 are experimentally factored to be 523 and 557.[127]

3.1. NMR realization for the HHL algorithm

Linear equations play an important role in all fields of sciences and engineering involving quantitative analysis. For example, in global positioning system (GPS), we have to

receive the signals from N satellites, then construct $(N-1)$-dimensional linear equations through geometric relationships and mathematical changes, and obtain the position by solving these equations. The experimental implementation of HHL algorithm was recently realized in NMR quantum processor,[72,128] which will be introduced in the following.

The algorithm of linear equations of N unknowns, even to obtain an approximate solution, in general requires time in the scale of at least N for a classical computer. One quantum algorithm purposed by Harrow *et al.* indicates that the HHL algorithm can solve an N-dimensional linear equation in $O(\log N)$ time which is as much as exponentially faster than the classical algorithms. Details of the HHL algorithm are introduced as follows.

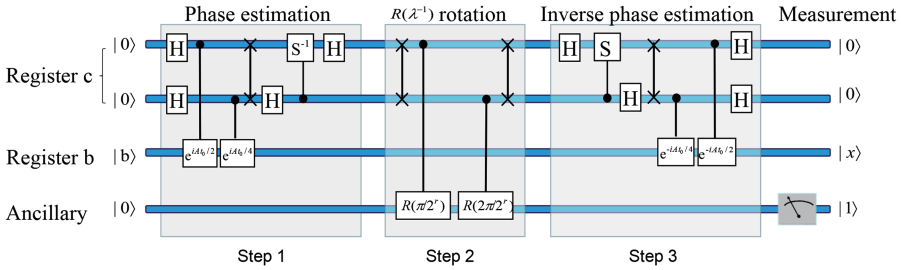


Fig. 4. (color online) Quantum circuit for implementing the HHL algorithm in NMR with $r=2$ and $t_0=2\pi$. Single-qubit operations S and H are respectively phase gate and Hadamard gate. $S=(1\ 0;0\ i)$, $H=(1\ 1;1\ -1)\sqrt{2}$. $R(\theta)$ is the rotation operation around y axis. $R(\theta)=(\cos(\theta/2)\ -\sin(\theta/2);\ \sin(\theta/2)\ \cos(\theta/2))$. The vertical segment with $\times$ means an SWAP operation.

Given a Hermitian $(N\times N)$ matrix $\boldsymbol{A}$ with a spectral decomposition $\boldsymbol{A}=\sum_{i=1}^{N}\lambda_i|u_i\rangle\langle u_i|$, where λ_i is the eigenvalue of $\boldsymbol{A}$ and $|u_i\rangle$ is the corresponding eigenstate and a unit vector $\boldsymbol{b}$. Then solving the linear equations is to find a vector $\boldsymbol{x}$ that satisfies $\boldsymbol{A}\boldsymbol{x}=\boldsymbol{b}$. In quantum language, $\boldsymbol{b}$ can be represented by a quantum state $|b\rangle=\sum_{i=1}^{N}b_i|i\rangle$. We can also expand $|b\rangle$ in the eigenbasis of $\boldsymbol{A}$ as $|b\rangle=\sum_j\beta_j|u_j\rangle$. If $\boldsymbol{A}$ is not Hermitian, we can further define

$$\boldsymbol{A}'=\begin{pmatrix}0 & \boldsymbol{A}\\ \boldsymbol{A}^{\dagger} & 0\end{pmatrix},\quad \boldsymbol{A}'\boldsymbol{y}=\begin{pmatrix}\boldsymbol{b}\\ 0\end{pmatrix},\quad \boldsymbol{y}=\begin{pmatrix}0\\ \boldsymbol{x}\end{pmatrix} \tag{24}$$

to make sure $\boldsymbol{A}'$ is Hermitian, such that we can solve Eq. (24) to obtain the $\boldsymbol{x}$ in quantum computing processor. We assume that $\boldsymbol{A}$ is Hermitian in the following. This algorithm needs an additional register c for the phase estimation and an ancillary qubit for the projective measurement, besieds the work qubits denoted by a register b which encodes a vector $\boldsymbol{b}$ and creates a desired vector $\boldsymbol{x}$. There are two main steps to solve this in quantum principle. First, use the well-known techniques of phase estimation with the controlled unitary $U=\sum_{\tau=0}^{T-1}|\tau\rangle\langle\tau|\otimes \mathrm{e}^{\mathrm{i}\boldsymbol{A}\tau t_0/T}$, where $T=2^l$ and $t_0=O(\kappa/\varepsilon)$, with l being the qubit number of register c. After this step, we can obtain the state of the registers c and b in the eigenbasis of $\boldsymbol{A}$, $\sum_i\beta_i|\lambda_i\rangle_C|u_i\rangle_B$. Second, an ancillary qubit is added to use the $|\lambda_j\rangle$ as a control register to obtain the state

$$\sum_i\left(\sqrt{1-\frac{C^2}{\lambda_i^2}}|0\rangle+\frac{C}{\lambda_i}|1\rangle\right)\beta_i|\lambda_i\rangle|u_i\rangle, \tag{25}$$

with an appropriate constant C. To realize the state transformation, we prepare the state $|\theta_i\rangle$ with $\theta_i=2\arcsin(C/\lambda_i)$ starting from $|\lambda_i\rangle$, and then use $|\theta_i\rangle$ as the control qubit to rotate the ancillary qubit. Finally, we perform the inverse phase estimation process and then obtain

$$\sum_i\left(\sqrt{1-\frac{C^2}{\lambda_i^2}}|0\rangle+\frac{C}{\lambda_i}|1\rangle\right)|0\rangle^{\otimes l}\beta_i|u_i\rangle. \tag{26}$$

When a projective measurement is applied on the ancilla qubit yielding $|1\rangle$ with certain probabilities, the state in register b will collapse to the desired state $\sum_i(C/\lambda_i)\beta_i|u_i\rangle$, which is actually the answer for $\boldsymbol{A}|x\rangle=|b\rangle$.

In experiments, Du *et al.* implemented the HHL algorithm using NMR quantum processor.[72] They chose iodotrifluoroethylene dissolved in d-chloroform as a four-qubit sample, where a ^{13}C nucleus and three ^{19}F nuclei constitute a four-qubit quantum system. The experiment can be divided into three steps as shown in Fig. 4. First, prepare the system into a pseudo-pure state (PPS), perform a rotation operation around the y axes with an angle θ to the third qubit, and obtain the initial state $\rho_0=|00\rangle\langle 00|\otimes|b\rangle\langle b|\otimes|0\rangle\langle 0|$, with the normalized state $|b\rangle=\cos(\theta/2)|0\rangle+\sin(\theta/2)|1\rangle$. For the simplification, they considered a specified matrix $\boldsymbol{A}$ as follows:

$$\begin{pmatrix}3 & 1\\ 1 & 3\end{pmatrix}. \tag{27}$$

Second, they implement the quantum circuit of the algorithm shown in Fig. 4 on the initial state ρ_0. All these operations are realized using an RF pulse which is optimized by the GRAPE technique. Finally, the single-qubit state tomography is carried out to read out the target vector $|x\rangle$ from the final state. It is the first experimental demonstration of the HHL algorithm when a (2×2) linear equation is considered using an NMR quantum information processor.

3.2. NMR realization for the applications on machine learning

Recently, the artificial intelligence and machine learning become more and more popular. Classical learning ma-

chines often require huge computational resources.[129] With the development of quantum technology, it is gradually known that a quantum machine learning algorithm may be exponentially faster than the classical counterparts with quantum parallelism for some special problems.[130,131] The participation of quantum computing injects a new driving force for conventional machine learning. Quantum principles can optimize the classical machine learning algorithms and improve the performance.[132,133] Therefore, one promising application of QIP is to combine the artificial intelligence and machine learning.

Many theoretical and experimental developments about machine learning in quantum information field have been achieved.[134–137] One of these is the experimental implementation of quantum version of the support vector machine (SVM). It is believed that SVM is a popular one and learns from training data and classifies vectors in a feature into one of two sets among the supervised machine learning algorithms.[136] Li *et al.* applied the SVM algorithm to the optical character recognition (OCR) problem.[137] It shows the ability to learn standard character fonts and then recognize handwritten characters from a set with two candidates. In detail, they took the printed images of the standard fonts of '6' and '9' as the training sets and classified the handwritten images of characters "6" and "9". As introduced before, the essential step of the SVM algorithm is the HHL algorithm. Thus the experiment process of SVM includes the HHL process, plus the additional two unitary operations which can be realized by the GRAPE techniques in NMR platform. The experimental results show that it can classify handwritten images of character "6" and "9" successfully.

4. Achievements for quantum simulation on NMR

As the real world obeys the rule of quantum mechanics, it should be described by the Hilbert space. However, as the size of the system increases, the traditional way for simulation becomes exponentially harder. An obvious challenge is to have a big memory to store a large state in the Hilbert space. Nowadays, the ability of the traditional CPU cannot drive a classical simulation of such evolution. Thirty years ago, Feynman once imagined to simulate the real physical phenomenon with a quantum system,[10] which is considered as one of the origins of concept of quantum computer right now. To some extent, a quantum computer is the universal quantum simulator.

In the area of QIP, one main purpose is to achieve the so called "quantum supremacy", which promises a certain realization on a quantum device that outperforms classical supercomputers. Quantum simulator, which is regarded as a quantum computer with certain aims, may touch this quantum supremacy in a few years. It is the first step to realize a universal quantum computer and some recent experiments have shed light on it.

Quantum simulators have been successfully implemented in several quantum platforms, such as trapped ions, photonics systems, and superconducting systems. NMR system, with its sixty years developments of quantum control techniques, could lead an unrivaled control on the system up to 12 qubits. Liquid-state NMR quantum information processing was first theoretically introduced independently by Cory *et al.* and Gershenfeld *et al.*[34,138] Due to the long decoherence time and accurate radio-frequency pulses, it is often seem as an outstanding platform for quantum simulation.[139–141] Since 2004, a set of experiments about simulating other physical systems were demonstrated. In 2004, Zhang *et al.* used a three-qubit nuclear magnetic resonance quantum system to implement the quantum clock synchronization algorithm based on quantum phase estimation.[74] In 2008, Zhang *et al.* studied the critical point in quantum phase transition and developed a technique by introducing a probe qubit, making the NMR system accessible to more complex simulation.[80] In 2009, Peng *et al.* mimic a Hamiltonian with two- and three-body interactions. They adiabatically prepared the ground states under such Hamiltonian. It opens a way to simulate a complex Hamiltonian in NMR system.[76] In 2010, an experimental realization of simulating a hydrogen molecule was reported by Du *et al*. Accurately they obtained its ground-state energy and showed the potential in calculations of quantum chemistry.[75] Following the hydrogen molecule simulation, another experiment simulating the chemical reaction was implemented.[142] In the same year, the localization effects induced by decoherence were simulated by Dieter Suter.[8] Some basic quantum problems were also simulated in NMR quantum simulator. In 2013, an experiment about simulation of quantum tunneling through potential barriers was reported by Feng *et al*. They showed that peculiar quantum phenomena could be studied with the use of quantum computers.[81] Recently, there are some intersection between biology and quantum information processing.[143,144] NMR quantum simulator could even be used to study some biology behaviors.

Nowadays, there are two other areas in which NMR quantum simulator are used: topological order[145–147] and high energy physics.[148,149] We will illustrate them in the following.

4.1. NMR platform for simulating the topological matter

Topological quantum computation (TQC) is one of the architectures of quantum computation, which was proposed by Alexei Kitaev.[146] The basic elements used in topological quantum computing are a kind of two-dimensional quasiparticles which are called anyons. Their braids are formed in a $(2+1)$-dimensional space by crossing their world lines and the unitary operations in TQC are generated by these braids. Compared with other quantum computing models, TQC has a natural advantage that the local errors have no influence on these braids, hence this architecture of quantum computation is invulnerable against small perturbations or errors. However, this fantastic and promising computation architecture still stays at theoretical realm since the basic elements of TQC in the real physical system are still difficult to be confirmed. The development of a controlled quantum device provides us with an alternative way to topological matter. In this way, we could simulate them in another quantum system rather than built it in a real physical system. For instance, the topological order between Abelian and non-Abelian can be efficiently simulated. Among the problems on research, one is to distinguish two kinds of topological orders. It is shown that a topological order can be uniquely determined by the following three factors: the anyon types, the topological properties, and the topological protected ground states. The anyon types and the topological protected ground states are equivalent on the torus, hence identification of a topological order merely depends on the topological properties of anyons which include self-statistics, braiding, and fusion. One of the common methods is to consider their modular S and T matrices, which provide the full information of the topological properties of anyons.

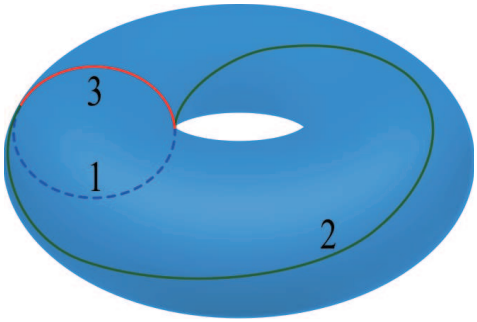


Fig. 5. (color online) The work is to simulate the minimal honeycomb lattice on a torus. This torus only contains one plaquette, two vertices, and three edges. 1,2,3 are three edges which can be simulated by three qubits, respectively.[150]

A recent experiment has shown that they could characterize topological orders and identify them via their modular $\boldsymbol{S}$ and $\boldsymbol{T}$ matrices using a three-qubit NMR quantum simulator (Fig. 5).[150] In their experiment, their three-qubit quantum system was loaded on the ^{13}C-labeled trichloroethylene (TCE) molecule which was dissolved in d-chloroform solvent. Three steps were adopted in their each experiment: preparation of the topological protected ground states, driving the system into a modular transformation, and measurement. Their experiment successfully simulated the states for Z_2 toric code, doubled semion order, and the doubled Fibonacci order and then identified them by experimental results. In the same period, Luo *et al.*[151] answered a new question "How much detail of the physics of topological orders can in principle be observed using state of the art technologies"? Based on a five-qubit NMR quantum simulator, which is represented by the 1-bromo-2,4,5-trifluorobenzene molecule, they adiabatically prepared the random ground state and measured the modular S and T matrices. They found that they could identify a Z_2 toric code model using a Hamiltonian with minimal input from state preparation to measurements. This is the first experiment which realizes the topological order and tests their robustness against perturbations. It may open a new territory to identify the topological orders whose Hamiltonians are not exactly solvable.

4.2. NMR platform for the problems in high energy physics

The other aspect lies on the area of high energy physics. Some other systems have proved that some high energy problems can be mimicked on a quantum simulator.[152] As for NMR quantum simulator, there are also some achievements about high energy physics simulation. Recently, they used an NMR quantum simulator, measuring holographic entanglement entropy, to mimic the Anti-de Sitter/conformal field theory (AdS/CFT) correspondence (Fig. 6).[153]

In classical spacetime, it is shown that physical variables commute with each other. However, some variables do not commute in quantum spacetime and as a result, these variables which use to be continuous may become discrete now. Quantum spacetime is such a generalization of the concept of spacetime that it is an area emerging quantum mechanics and general relativity. At present, there are two mainstream approaches by expanding either quantum mechanics or general relativity to investigate it. First, the famous string theory is constructed by considering the gravity in quantum field theory, to finally become a theory of quantum gravity. Second, as the leading competitor to string theory, loop quantum gravity (LQG) begins with relativity and tries to add quantum properties. In the past two decades, AdS/CFT correspondence is one of the most important conjectured relationship to quantum theory of gravity. It predicts that the quantum gravity theory in the bulk anti-de Sitter spacetime has an equivalent relation to the conformal field theories which are from quantum field

theories on a lower-dimensional space.

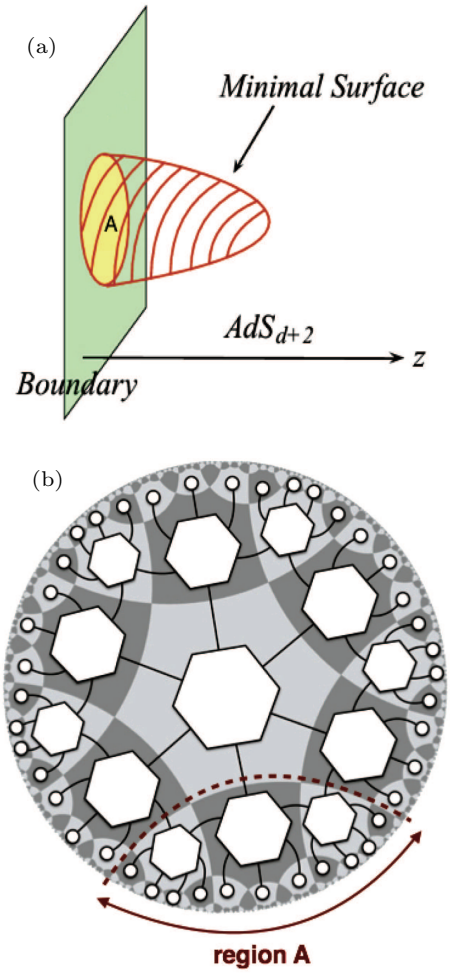


Fig. 6. (color online) Description of the RT formula. The bulk minimal surface (blue line) is anchored at the boundary of the boundary region A. (b) An example of tensor network state. The (hexagon) nodes represent tensors. The links represent the contraction of tensors. The dangling legs are physical DOFs in many-body system. The red dashed curve illustrates the virtual surface S anchored to region A, which cuts a minimal number of links.[153]

Starting from the entanglement in the boundary field theory, Li *et al.* rebuilt the bulk geometry holographically. To identify the entanglement entropy $S_{\mathrm{EE}}(A)$, the Ryu–Takayanagi (RT) formula was proposed

$$S_{\mathrm{EE}}(A) = \frac{Ar_{\min}}{4G_{\mathrm{N}}}, \tag{28}$$

where G_{N} is the Newton constant. A is a $(d-1)$-dimensional boundary region, with the bulk $(d-2)$-dimensional minimal surface $Ar_{\min}$ anchored to A. On the other hand, recent prosperous area called tensor network has introduced a way making the RT formula a discrete version. With the assist of the above developments, the quantum simulator will become available for the implementation of these demonstrations. For instance, a six-qubit NMR quantum simulator was recently adopted to realize such a demonstration. The spin-half ^{13}C in ^{13}C-labeled dichloro-cyclobutanone dissolved in d6-acetone was regarded as six qubits. They used control techniques include GRAPE and a pulse feedback program to boost the accuracy of the RF pulses. Experiments successfully presented the simulation of the minimal PT of rank-6. Although they just implemented the minimum case for the RT formula, their results further suggest that the RT formula or the AdS/CFT correspondence can be simulated on a larger quantum system.

Towards quantum gravity, loop quantum gravity leads another description of the quantum spacetime. In the frame of LQG, at a certain time point, the geometry can be thought as concentrating on one-dimensional structures. It is simply a one-dimensional oriented network, which is a so-called spin network. It was first proposed by Penrose and the oriented lines are linked together at their end points to form a whole net. In the spin-network, quantum spacetime can be decomposed into some kind of quantum tetrahedron. This tetrahedron corresponds to a certain state and can also be simulated in current quantum devices such as NMR quantum simulator platform. Additionally, some endeavors could be made to simulate their dynamics if more qubits could be controlled. Moreover, the NMR platform can also be used to simulate other relevant models such as a black hole which could be seen as quantum scrambling in a chaotic system,[154,155] the Sachdev–Ye–Kitaev model,[156] and the space–time geometry emerged from entanglement.[157]

5. Conclusion and perspectives

The above description of QIP clearly shows that quantum devices come into being a next generation information processor which could bring us more powerful computing power than existing classical computers. The road of constructing a practical universal quantum computer is a hard task, but this goal will be finally achieved after the painstaking endeavors of many scientists and engineers in the experimental implementations of QIP. In the mid-development, it may be a possible approach that quantum and classical processors are combined together to form a hybrid computer.

Although so many quantum control techniques are developed and the theoretical quantum algorithms and quantum computing are successfully demonstrated in the experiments in liquid-state NMR, there are still natural limitations such as the non-scalability, the inability for resetting qubits, and the long time of implementing quantum gates. As the first generation and pioneer of realizing QIP experimentally, it is believed that liquid-state NMR still plays an important role in the future program towards an universal quantum computer. First, liquid-state NMR has plentiful of successful techniques for demonstrating QIP. The theory and techniques obtained in NMR can

be transferred to and used by other quantum systems in order to precisely realize quantum gate operations. Hence, liquid-state NMR will be a reliable testbed in the future development of QIP. Second, NMR is still an outstanding system for simulating complex multi-body dynamics which is usually unaccessible for other systems in the current technology. Third, there are still many potential techniques to be developed in NMR which can provide experience and guidance for other potential QIP systems.

Besides, it is fortunate that the new generation of NMR platform based on crystals and solids can be further established which will overcome many of the existing limitations in liquid-state NMR. Solid-state NMR for QIP brings four advantages: (i) high polarization for increasing the sensitivity; (ii) longer coherent time to make it possible to demonstrate complex and interesting algorithms; (iii) stronger coupling between spins to reduce the time of quantum gates operations; (iv) resetting qubits. Hence, solid-state NMR provides a new opportunity to explore a new territory for QIP.

References

[1] Bennett C H and DiVincenzo D P 2000 *Nature* **404** 6775
[2] Schwindt P D D, Kwiat P G and Englert B G 1999 *Phys. Rev. A* **60** 4285
[3] Long G L 2006 *Commun. Theor. Phys.* **45** 825
[4] Horodecki R, Horodecki P, Horodecki M and Horodecki K 2009 *Rev. Mod. Phys.* **81** 865
[5] Guo R, Zhou L, Gu S P, *et al*. 2016 *Chin. Phys. B* **25** 030302
[6] Friedman J R, Patel V, Chen W, Tolpygo S K and Lukens J E 2000 *Nature* **406** 6791
[7] Li T and Yin Z Q 2016 *Sci. Bull.* **61** 163
[8] Benioff P 1980 *J. Stat.Phys.* **22** 563
[9] Deutsch D 1985 *Proc. R. Soc. Lond. A* **400** 97
[10] Feynman R P 1982 *Int. J. Theor. Phys.* **21** 476
[11] Deng F G, Long G L and Liu X S 2003 *Phys. Rev. A* **68** 042317
[12] Deng F G and Long G L 2004 *Phys. Rev. A* **69** 052319
[13] Zhao X L, Li J L, Niu P H, *et al*. 2017 *Chin. Phys. B* **26** 030302
[14] Yan C, Shi Z, Li Y, *et al*. 2016 *Chin. Phys. B* **24** 050307
[15] Shor P W 1999 *SIAM Rev.* **41** 303
[16] Knill E 2010 *Nature* **463** 441
[17] Ahn J, Weinacht T C and Bucksbaum P H 2000 *Science* **287** 5452
[18] DiVincenzo D P 2000 arXiv: 0002077 [quant-ph]
[19] Jones J A, Vedral V, Ekert A and Castagnoli G 1999 arXiv: 9910052 [quant-ph]
[20] Shnirman A, Schon G and Hermon Z 1997 *Phys. Rev. Lett.* **79** 2371
[21] Chiorescu I, Nakamura Y, Harmans C M and Mooij J E 2003 *Science* **299** 5614 1869
[22] Cirac J I and Zoller P 1995 *Phys. Rev. Lett.* **74** 4091
[23] Kielpinski D, Monroe C and Wineland D J 2002 *Nature* **417** 709
[24] Imamog A, Awschalom D D, Burkard G, DiVincenzo D P, Loss D, Sherwin M and Small A 1999 *Phys. Rev. Lett.* **83** 4204
[25] Pellizzari T, Gardiner S A, Cirac J I and Zoller P 1995 *Phys. Rev. Lett.* **75** 3788
[26] Kok P, Munro W J, Nemoto K, Ralph T C, Dowling J P and Milburn G J 2007 *Rev. Mod. Phys.* **79** 135
[27] Obrien J L 2007 *Science* **318** 1567
[28] Li A X, Duan S Q and Zhang W 2016 *Chin. Phys. B* **25** 108506
[29] Loss D and DiVincenzo D P 1998 *Phys. Rev. A* **57** 120
[30] Petta J R, Johnson A C, Taylor J M, Laird E A, Yacoby A, Lukin M D and Gossard A C 2007 *Science* **309** 2180
[31] Rigden J S 1986 *Rev. Mod. Phys.* **58** 433
[32] Chuang I L, Gershenfeld N, Kubinec M G and Leung D W 1998 *Proc. R. Soc. Lond. A* **454** 447
[33] Knill E and Laflamme R 1998 *Phys. Rev. Lett.* **81** 5672
[34] Cory D G, Fahmy A F and Havel T F 1997 *Proc. R. Soc. A* **94** 1634
[35] Cory D G, Laflamme R, Knill E, Viola L, Havel T F and Boulant N 2000 *Fortschritte der Physik* **48** 875
[36] Cory D G, Price M D and Havel T F 1998 *Physica D* **120** 82
[37] Vandersypen L M and Chuang I L 2005 *Rev. Mod. Phys.* **76** 1037
[38] Zhen X L, Xin T, Zhang F H and Long G L 2016 *Sci. China-Phys., Mech. & Astron.* **59** 690312
[39] Pan X Y 2016 *Sci. China-Phys., Mech. & Astron.* **60** 020333
[40] Brown K R, Harrow A W and Chuang I L 2004 *Phys. Rev. A* **70** 052318
[41] Alway W G and Jones J A 2007 *Phys. Rev. A* **189** 114
[42] Fung B M, Khitrin A K and Ermolaev K 2000 *J. Magn. Reson.* **142** 97
[43] Waugh J S, Huber L M and Haeberlen U 1968 *Phys. Rev. Lett.* **20** 180
[44] Shaka A J, Keeler J, Frenkiel T and Freeman R A Y 1983 *J. Magn. Reson.* **52** 335
[45] Viola L, Knill E and Lloyd S 1999 *Phys. Rev. Lett.* **82** 2417
[46] Souza A M, Alvarez G A and Suter D 2011 *Phys. Rev. Lett.* **106** 240501
[47] Zhen X L, Zhang F H, Feng G, Li, H and Long G L 2016 *Phys. Rev. A* **93** 022304
[48] Zhang J, Souza A M, Brandao F D and Suter D 2014 *Phys. Rev. Lett.* **112** 050502
[49] West J R, Lidar D A, Fong B H and Gyure M F 2010 *Phys. Rev. Lett.* **105** 230503
[50] Aharonov D, Van Dam,W, Kempe J, Landau Z, Lloyd S and Regev O 2008 *SIAM Rev.* **50** 755
[51] Childs A M, Farhi E and Preskill J 2001 *Phys. Rev. A* **65** 012322
[52] Gaitan F and Clark L 2012 *Phys. Rev. Lett.* **108** 010501
[53] Stoustrup J, Schedletzky O, Glaser S J, Griesinger C, Nielsen N C and Sorensen O W 1995 *Phys. Rev. Lett.* **74** 2921
[54] Fortunato E M, Pravia M A, Boulant N, Teklemariam G, Havel T F and Cory D G 2002 *J. Chem. Phys.* **116** 7599
[55] Boulant N, Edmonds K, Yang J, Pravia M A and Cory D G 2002 *Phys. Rev. A* **68** 032305
[56] Khaneja N, Reiss T, Kehlet C, Schulte-Herbruggen T and Glaser S J 2005 *J. Magn. Reson.* **172** 296
[57] Li J, Yang X, Peng X and Sun C P 2016 arXiv: 1608.00677
[58] Lu D, Li K, Li J, Katiyar H, Park A J and Feng G 2017 arXiv: 1701.01198
[59] Rebentrost P, Schuld M, Petruccione F and Lloyd S 2016 arXiv: 1612.01789
[60] Egger D J and Wilhelm F K 2014 *Supercond. Sci. & Technol.* **27** 014001
[61] Ryan C A, Negrevergne C, Laforest M, Knill E and Laflamme R 2008 *Phys. Rev. A* **78** 012328
[62] Knill E, Laflamme R, Martinez R and Tseng C H 2000 *Nature* **404** 368
[63] Li J, Cui J, Laflamme R and Peng X 2016 *Phys. Rev. A* **94** 032316
[64] Xin T, Lu D, Klassen J, Yu N, Ji Z and Chen J 2017 *Phys. Rev. Lett.* **118** 020401
[65] Jonathan A. Jones J A, Mosca M and Hansen R H 1998 *Nature* **393** 344
[66] Long G L 2001 *Phys. Rev. A* **64** 022307
[67] Liu Y and Zhang F 2015 *Sci. China-Phys., Mech. & Astron.* **58** 1
[68] Vandersypen L M, Steffen M, Breyta G, Yannoni C S, Sherwood M H and Chuang I L 2001 *Nature* **414** 883
[69] Chuang I L, Vandersypen L M K, Zhou X, Leung D W and Lloyd S 1998 *Nature* **393** 143
[70] Vandersypen L M, Steffen M, Breyta G, Yannoni C S, Cleve R and Chuang I L 2000 *Phys. Rev. Lett.* **85** 5452
[71] Peng X, Zhu X, Fang X, Feng M, Liu M and Gao K 2002 *Phys. Rev. A* **65** 042315
[72] Pan J, Cao Y, Yao X, Li Z, Ju C and Chen H 2014 *Phys. Rev. A* **89** 022313
[73] Georgescu I M, Ashhab S and Nori F 2014 *Rev. Mod. Phys.* **86** 153
[74] Zhang J, Long G L, Deng Z, Liu W and Lu Z 2004 *Phys. Rev. A* **70** 062322
[75] Du J, Xu N, Peng X, Wang P, Wu S and Lu D 2010 *Phys. Rev. Lett.* **104** 030502
[76] Peng X, Zhang J, Du J and Suter D 2009 *Phys. Rev. Lett.* **103** 140501
[77] Alvarez G A and Suter D 2010 *Phys. Rev. Lett.* **104** 230403
[78] Alvarez G A, Suter D and Kaiser R 2015 *Science* **349** 846
[79] Peng X, Du J and Suter D 2005 *Phys. Rev. A* **71** 012307
[80] Zhang J, Peng X, Rajendran N and Suter D 2008 *Phys. Rev. Lett.* **100** 100501

[81] Feng G R, Lu Y, Hao L, Zhang F H and Long G L 2013 *Sci. Rep.* **3**
[82] Zheng C, Hao L and Long G L 2013 *Phil. Trans. R. Soc. A* **371** 20120053
[83] Nielsen M A, Knill E and Laflamme R 1998 *Nature* **396** 52
[84] Fang X, Zhu X, Feng M, Mao X A and Du F 2000 *Phys. Rev. A* **61** 022307
[85] Roy S S, Shukla A and Mahesh T S 2012 *Phys. Rev. A* **85** 022109
[86] Souza A M, Magalhaes A, Teles J, Bonagamba T J, Oliveira I S and Sarthour R S 2008 *New J. Phys.* **10** 033020
[87] Souza A M, Oliveira I S and Sarthour R S 2011 *New J. Phys.* **13** 053023
[88] Xin T, Li H, Wang B X and Long G L 2015 *Phys. Rev. A* **92** 022126
[89] Wei S J and Long G L 2016 *Quantum Inf. Process.* **15** 1189
[90] Hou S Y, Li H and Long G L 2017 *Sci. Bull.* **62** 863
[91] Li H, Gao X, Xin T, Yung M H and Long G L 2015 *Sci. Bull.* **62** 497
[92] Lu D, Li H, Trottier D A, Li J, Brodutch A and Krismanich A P 2015 *Phys. Rev. Lett.* **114** 140505
[93] Lu D, Xin T, Yu N, Ji Z, Chen J and Long G 2016 *Phys. Rev. Lett.* **116** 230501
[94] Feng G, Xu G and Long G 2013 *Phys. Rev. Lett.* **110** 190501
[95] Li H, Liu Y and Long G 2017 *Sci. China-Phys., Mech. & Astron.* **60** 080311
[96] Levitt M H 2008 *Spin Dynamics: Basics of NMR*
[97] Suter D and Mahesh T S 2008 *J. Chem. Phys.* **128** 052206
[98] Wiseman H M and Milburn G J 2009 *Quantum Measurement and Control* (Cambridge: Cambridge University Press)
[99] Nielsen M and Chuang I 2000 *Quantum Information and Computation*
[100] Mansfield P 1970 *Phys. Lett. A* **32** 485
[101] Khodjasteh K, Sastrawan J, Hayes D, *et al.* 2013 *Nat. Commun.* **4**
[102] Biercuk M J, Doherty A C and Uys H 2011 *J. Phys. B: At. Mol. Opt. Phys.* **44** 154002
[103] Hahn E L 1950 *Phys. Rev.* **80** 580
[104] Viola L and Lloyd S 1998 *Phys. Rev. A* **58** 2733
[105] Carr H Y and Purcell E M 1954 *Phys. Rev.* **94** 630
[106] Meiboom S and Gill D 1958 *Rev. Sci. Instrum.* **29** 688
[107] Uhrig G S 2007 *Phys. Rev. Lett.* **98** 100504
[108] Uhrig G S 2008 *New J. Phys.* **10** 083024
[109] Du J, Rong Z, Zhao N, Wang Y, Yang J and Liu R 2009 *Nature* **461** 1265
[110] Biercuk M J, Uys H, VanDevender A P, *et al.* 2009 *Nature* **458** 996
[111] Biercuk M J, Uys H, VanDevender A P, *et al.* 2009 *Phys. Rev. A* **79** 062324
[112] Khodjasteh K and Lidar D 2005 *Phys .Rev. Lett.* **95** 180501
[113] West J R, Fong B H and Lidar D A 2010 *Phys. Rev. Lett.* **104** 130501
[114] Kuo W and Lidar D A 2011 *Phys. Rev. A* **84** 042329
[115] Jiang L and Imambekov A 2011 *Phys. Rev. A* **84** 060302
[116] Ai Q, Yen T, Jin B and Cheng Y 2013 *J. Phys. Chem. Lett.* **4** 2577
[117] Jing J, Wu L, Yu T, You J, Wang Z and Garcia L 2014 *Phys. Rev. A* **89** 032110
[118] Soare A, Ball H, Hayes D, Sastrawan J, Jarratt M C, McLoughlin J J, Zhen X, Green T J and Biercuk M J 2014 *Nat. Phys.* **10** 825
[119] Soare A, Ball H, Hayes D, Zhen X, Jarratt M C, Sastrawan J, Uys H and Biercuk M J 2014 *Phys. Rev. A* **89** 042329
[120] Shor P W 1999 *SIAM Rev.* **41** 303
[121] Lu C Y, Browne D E, Yang T and Pan J W 2007 *Phys. Rev. Lett.* **99** 250504
[122] Lanyon B P, Weinhold T J, Langford N K, Barbieri M, James D F V, Gilchrist A and White A G 2007 *Phys. Rev. Lett.* **99** 250505
[123] Politi A, Matthews J C and Obrien J L 2009 *Science* **325** 1221
[124] Monz T, Nigg D, Martinez E A, Brandl M F, Schindler P and Rines R 2016 *Science* **351** 1068
[125] Shor P W 2012 *Nat. Photon.* **6** 773
[126] Xu N, Zhu J, Lu D, Zhou X, Peng X and Du J 2012 *Phys. Rev. Lett.* **108** 130501
[127] Martin-Lopez E, Laing A, Lawson T, Alvarez R, Zhou X Q and Obrien J L 2017 arXiv: 1706.08061 [quant-ph]
[128] Harrow A W, Hassidim A and Lloyd S 2009 *Phys. Rev. Lett.* **103** 150502
[129] Michalski R S, Carbonell J G and Mitchell T M 2013 *Springer Science and Business Media*
[130] Schuld M, Sinayskiy I and Petruccione F 2015 *Contemporary Physics* **56** 172
[131] Biamonte J, Wittek P, Pancotti N, Rebentrost P, Wiebe N and Lloyd S 2016 arXiv: 1611.09347 [quant-ph]
[132] Lloyd S, Mohseni M and Rebentrost P 2013 arXiv: 1307.0411 [quant-ph]
[133] Wiebe N, Kapoor A and Svore K M 2015 *Quantum Inf. Comput.* **15**
[134] Cai X D, Wu D, Su Z E, Chen M C, Wang X L and Li L 2015 *Phys. Rev. Lett.* **114** 110504
[135] Dunjko V, Taylor J M and Briegel H J 2016 *Phys. Rev. Lett.* **117** 130501
[136] Rebentrost P, Mohseni M and Lloyd S 2014 *Phys. Rev. Lett.* **113** 130503
[137] Li Z, Liu X, Xu N and Du J 2015 *Phys. Rev. Lett.* **114** 140504
[138] Gershenfeld N A and Chuang I L 1997 *Science* **275** 350
[139] Lu Y, Feng G R, Li Y S and Long G L 2015 *Sci. Bull.* **60** 241
[140] Pearson J, Feng G, Zheng C and Long G 2015 *Sci. China-Phys., Mech. & Astron.* **59** 120312
[141] Jin F, Chen H, Rong X, Zhou H, Shi M and Zhang Q 2015 *Sci. China-Phys., Mech. & Astron.* **59** 630302
[142] Lu D, Xu N, Xu R, Chen H, Gong J, Peng X and Du J 2011 *Phys. Rev. Lett.* **107** 020501
[143] Alvarez-Rodriguez U, Sanz M, Lamata L and Solano E 2016 *Sci. Rep.* **6**
[144] Alvarez-Rodriguez U, Sanz M, Lamata L and Solano E 2014 *Sci. Rep.* **4**
[145] Nayak C, Simon S H, Stern A, Freedman M and Sarma S D 2008 *Rev. Mod. Phys.* **80** 1083
[146] Kitaev A Y 2003 *Ann. Phys.* **303** 2
[147] Park A J, McKay E, Lu D and Laflamme R 2016 *New J. Phys.* **18** 043043
[148] Li J, Fan R, Wang H, Ye B, Zeng B and Zhai H 2017 *Phys. Rev. X* **7** 031011
[149] Swingle B, Bentsen G, Schleier-Smith M and Hayden P 2016 *Phys. Rev. A* **94** 040301
[150] Li K, Wan Y, Hung L Y, Lan T, Long G and Lu D 2017 *Phys. Rev. Lett.* **118** 080502
[151] Luo Z, Li J, Li Z, Hung L Y, Wan Y, Peng X and Du J 2016 arXiv: 1608.06978 [quant-ph]
[152] Martinez E A, Muschi C A, Schindler P, Nigg D, Erhard A, Heyl M, Hauke P, Dalmonte M, Monz T, Zoller P and Blatt R 2016 *Nature* **534** 516
[153] Li K, Han M, Long G, Wan Y, Lu D, Zeng B and Laflamme R 2017 arXiv: 1705.00365 [quant-ph]
[154] Maldacena J, Shenker S H and Stanford D 2016 *J. High Energy Phys.* **2016** 106
[155] Hosur P, Qi X L, Roberts D A and Yoshida B 2016 *J. High Energy Phys.* **2016** 4
[156] Sachdev S and Ye J 1993 *Phys. Rev. Lett.* **70** 3339
[157] Ryu S and Takayanagi T 2006 *Phys. Rev. Lett.* **96** 181602